Noise control zone for a periodic ducted Helmholtz resonator system

Chenzhi Cai and Cheuk Ming Mak

Citation: The Journal of the Acoustical Society of America **140**, EL471 (2016); doi: 10.1121/1.4968530
View online: https://doi.org/10.1121/1.4968530
View Table of Contents: https://asa.scitation.org/toc/jas/140/6
Published by the Acoustical Society of America

Chenzhi Cai and Cheuk Ming Mak: JASA Express Letters [http://dx.doi.org/10.1121/1.4968530] Published Online 1 December 2016

Noise control zone for a periodic ducted Helmholtz resonator system

Chenzhi Cai and Cheuk Ming Mak[a)]
Department of Building Services Engineering, The Hong Kong Polytechnic University, Hung Hom, Kowloon, Hong Kong, China
chenzhi.cai@connect.polyu.hk, cheuk-ming.mak@polyu.edu.hk

Abstract: This paper presents a theoretical study of the dispersion characteristics of sound wave propagation in a periodic ducted Helmholtz resonator (HR) system. The predicted result fits well with a numerical simulation using a finite element method. This study indicates that for the same system, no matter how many HRs are connected or what the periodic distance is, the area under average transmission loss $\overline{TL}$ curves is always the same. The broader the noise attenuation band, the lower the peak attenuation amplitude. A noise control zone compromising the attenuation bandwidth or peak amplitude is proposed for noise control optimization.

Date Received: July 13, 2016 **Date Accepted:** November 4, 2016

1. Introduction

The Helmholtz resonator (HR), which consists of a cavity communicating with an external duct through a neck, is widely used to reduce low-frequency noise in a narrow frequency band at its resonance peak. The resonance frequency is only determined by the physical geometries of the cavity and the neck. It is therefore possible to design a silencer with a desired resonance frequency. The classical approach to modeling HRs considers an equivalent spring-mass system with end-correction factors for the sake of accuracy.[1,2] Furthermore, wave propagation in both duct and resonator has been considered in theoretical analysis. The one-dimensional wave propagation approach was considered in preliminary investigations and was expanded to a multidimensional approach in order to account for nonplanar effects. The latter has been proven by experiment to be a better theoretical analysis approach.[3–6]

Since a single resonator has a narrow noise attenuation band, an array of resonators is one way to obtain a broader noise attenuation band. Multiple-resonator arrays have been investigated to broaden the noise attenuation band in the low-frequency range.[7–10] Some researchers have discussed the acoustic performance of periodic ducted HR systems and proposed theoretical methods of predicting the bandwidth of the noise attenuation band. However, periodic ducted HR systems struggle to obtain the necessary broad attenuation bandwidth and high-peak attenuation amplitude at the same time.[11,12] A parameter based on the transmission loss index is first proposed here to investigate HRs' sound energy storage capacity. The parameter remains the same for the same geometries of duct and resonator. This clearly imposes limitations on noise control. A noise control zone compromising the attenuation bandwidth or peak amplitude of the periodic ducted HR system is also first proposed for noise control optimization.

2. Dispersion relation of sound waves in a periodic acoustic system

The sound waves propagated in a periodic ducted HR system are known as Bloch waves.[11,13] Only planar waves are considered in duct propagation because the frequency range considered here is well below the duct's cutoff frequency. Bloch wave theory and the transfer matrix method are used to investigate the dispersion relation of sound waves in a duct resonator system.

2.1 A duct with an array of Helmholtz resonators

Although a multidimensional approach provides a more accurate measure of the acoustic impedance of a resonator, the main purpose here is to reveal the dispersion relation of sound waves in a periodic ducted HR system. For this reason, the classical

[a)]Author to whom correspondence should be addressed.

approach is adopted here and the acoustic impedance of the resonator is expressed as[2,12]

$$Z_r = j\frac{\rho_0 l_n'}{S_n\omega}\left(\omega^2 - \omega_0^2\right), \tag{1}$$

where ρ_0 is air density, l_n' and S_n are the neck's effective length and area, respectively, and ω_0 and ω are the resonant circular frequency and circular frequency, respectively.

A duct segment with a resonator constitutes a typical periodic cell. The duct segment's length is regarded as a periodic distance based on the assumption that the diameter of the resonator's neck is negligible in a periodic cell. The sound pressure and particle velocity in the duct segment of the nth cell, as shown in Fig. 1, can be described as $p_n(x)$ and $u_n(x)$ with a suffix of n. The sound pressure is a combination of two wave propagations in opposite directions of axial x. Assuming a time-harmonic disturbance in the form of $e^{j\omega t}$, the sound pressure can be expressed as[1]

$$p_n(x) = I_n e^{-jk(x-x_n-\omega t)} + R_n e^{jk(x-x_n+\omega t)}, \tag{2}$$

where k is the number of waves, $x_n = (n-1)d$ represents the local coordinates, d is the periodic distance, and I_n and R_n represent respective complex wave amplitudes. Combining the continuity of sound pressure and volume velocity at $x = nd$ yields

$$\begin{bmatrix} I_{n+1} \\ R_{n+1} \end{bmatrix} = \begin{bmatrix} \left(1 - \frac{Z_d}{2Z_r}\right)\exp(-jkd) & -\frac{Z_d}{2Z_r}\exp(jkd) \\ \frac{Z_d}{2Z_r}\exp(-jkd) & \left(1 + \frac{Z_d}{2Z_r}\right)\exp(jkd) \end{bmatrix} \begin{bmatrix} I_n \\ R_n \end{bmatrix} = \mathbf{T}\begin{bmatrix} I_n \\ R_n \end{bmatrix}, \tag{3}$$

where Z_d is the acoustic impedance of the duct and $\mathbf{T}$ is the transfer matrix. Once the initial sound pressure is given, the sound pressure and particle velocity in an arbitrary cell can be determined successively using Eq. (3). According to Bloch wave theory, the transfer matrix can be set as $\mathbf{T} = \lambda$ [λ is set to be $\exp(-jqd)$ and q is the Bloch wave number and is allowed to be a complex value].

The analysis of the periodic structure translates to an eigenvalue and its corresponding eigenvector problem. From the definition of λ, q must satisfy the following dispersion relation:

$$\cos(qd) = \cos(kd) + j\frac{Z_d}{2Z_r}\sin(kd) = \cos(kd) + \frac{\psi kd\sin(kd)}{2\left[(\omega/\omega_0)^2 - 1\right]}, \tag{4}$$

where $\psi = V_c/S_d d$ (V_c represents the HR's volume and S_d the cross-sectional area of the duct). The Bloch wave number q is a complex value comprising a real part, q_r, and imaginary part, q_i; the solutions of $\lambda = \exp(-jqd)$ describe the propagation properties of Bloch waves. Assuming that $q_r > 0$ and $q_i > 0$, the two solutions $q = q_r - jq_i$ and $q = -(q_r - jq_i)$ represent the propagation properties of positive-x and negative-x Bloch waves, respectively, corresponding to the eigenvalues λ_1 and λ_2. The eigenvectors corresponding to eigenvalues λ_1 and λ_2 can be expressed as $[v_{I1}, v_{R1}]^{\mathbf{T}}$ and $[v_{I2}, v_{R2}]^{\mathbf{T}}$, respectively.

2.2 Dispersion relation

The solution of q is a function of the wave frequency, periodic distance, and geometric dimensions of a duct resonator system. The dispersion relation of sound waves in a duct can be described by solutions of q. When q contains an imaginary part, this

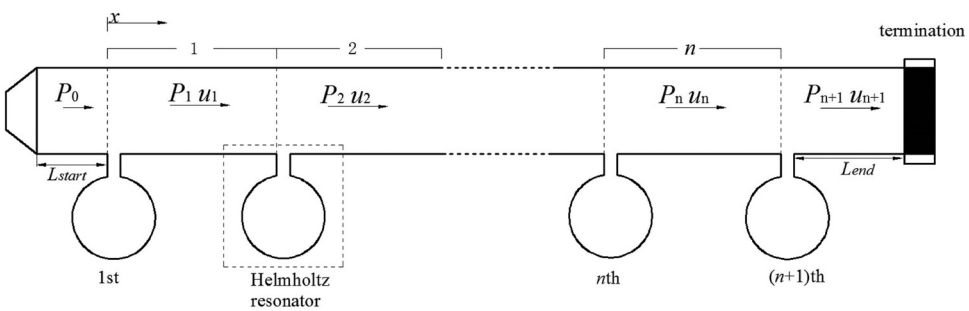

Fig. 1. Schematic diagram of a periodic ducted HR system with finite resonators.

implies that a sound wave decays as it travels; the frequency ranges of such a sound wave are called stopbands. Passbands are sound waves that have only a phase delay during travel when q only contains a real part. Stopbands are brought about physically by two mechanisms. One is when sound wave frequency coincides with the resonator's resonance frequency, which is also the mechanism of a single-resonator case. The other is Bragg reflection. Based on these two mechanisms, a theoretical prediction of stopband position and its bandwidth is studied.

When the asymptotic wave frequency $\omega \to \omega_0$ is considered, setting $\omega/\omega_0 = 1 + \Delta$ ($|\Delta|$ is assumed to be well below unity). When Eq. (4) is set to be unity, the approximate stopbands at $\Delta = \Delta_+$ and $\Delta = \Delta_-$ are expressed in the form of Taylor series,

$$\Delta_+ = \frac{V_c k_0}{4S_d}\left[\cot\left(\frac{k_0 d}{2}\right) + \frac{\cot'(k_0 d/2)}{1!}\frac{k_0 d}{2}\Delta_+ + \cdots + \frac{\cot^{(n)}(k_0 d/2)}{n!}\frac{k_0 d}{2}\Delta_+\right], \quad (5)$$

$$\Delta_- = -\frac{V_c k_0}{4S_d}\left[\tan\left(\frac{k_0 d}{2}\right) + \frac{\tan'(k_0 d/2)}{1!}\frac{k_0 d}{2}\Delta_- + \cdots + \frac{\tan^{(n)}(k_0 d/2)}{n!}\frac{k_0 d}{2}\Delta_-\right], \quad (6)$$

where $k_0 = \omega_0/c_0$ is the wave number of resonance frequency and c_0 is the sound velocity. The stopband of resonance can be expressed as $[(1+\Delta_-)\omega_0, (1+\Delta_+)\omega_0]$. For the sake of simplicity, when only zero-order correction is considered, the bandwidth is given as $\Delta_{bw} = V_c k_0 \omega_0 |\cot(k_0 d/2) + \tan(k_0 d/2)|/4S_d$.

The stopband is also due to Bragg reflection; it occurs near $\omega_m = m\pi c_0/d$ (m is an integer). Then $kd = m\pi$ (m is an integer) can be obtained, indicating the approximate positions of stopbands. When the asymptotic wave frequency $\omega \to \omega_m$ is considered, setting $\omega/\omega_m = 1 + \Delta$. Then, Eq. (4) is rewritten as[11]

$$\begin{aligned}\cos(qd) &= \cos(m\pi(1+\Delta)) + \frac{\psi m\pi(1+\Delta)\sin(m\pi(1+\Delta))}{2\left[\left(\omega_m(1+\Delta)/\omega_0\right)^2 - 1\right]} \\ &= (-1)^m\left[1 - \frac{(m\pi)^2}{2}\left(\Delta^2 - \Delta\Delta_m\right)\right]. \end{aligned} \quad (7)$$

Thus stopbands of Bragg reflection appear at $[(1-\Delta_m/2)\omega_m, (1+\Delta_m/2)\omega_m]$, where $\Delta_{bw} = \omega_m\Delta_m = \psi\omega_m/|(\omega_m/\omega_0)^2 - 1|$ represents the bandwidth. As the integer number m increases, the width of the stopband becomes narrower as $1/m^2$ and the maximum value of the imaginary part becomes smaller as $1/m$.[12]

In practice, the special case where the designed resonance frequency ω_0 coincides with the Bragg reflection frequency ω_m is applied to achieve a broader noise stopband at resonance frequency. The stopband is thus a combination of resonance and Bragg reflection. Then Eq. (7) is converted to $\cos(qd) = (-1)^m[1 - (m\pi)^2(\Delta^2 - \psi/2)/2]$. Thus, the stopband of the special case can be obtained at $[(1-\sqrt{\psi/2})\omega_0, (1+\sqrt{\psi/2})\omega_0]$, with bandwidth $\Delta_{bm} = 2\omega_0\sqrt{\psi/2}$. The bandwidth decreases with increasing $d (d = m\lambda_0/2)$, where $\lambda_0 = 2\pi c_0/\omega_0$ is the wavelength of resonance frequency. For the sake of a broader stopband at resonance frequency, $d = \lambda_0/2$ is often chosen as a periodic distance.

3. A parameter to evaluate the capacity of sound power storage in resonators

3.1 Transmission loss of periodic ducted HR systems

According to the definition of the eigenvalue, Eq. (3) can be expressed in eigenvector form as[13]

$$\begin{bmatrix} I_{n+1} \\ R_{n+1} \end{bmatrix} = \mathbf{T}\begin{bmatrix} I_n \\ R_n \end{bmatrix} = \mathbf{T}^2\begin{bmatrix} I_{n-1} \\ R_{n-1} \end{bmatrix} = \cdots = \mathbf{T}^n\begin{bmatrix} I_1 \\ R_1 \end{bmatrix} = A_0\lambda_1^n\begin{bmatrix} v_{I1} \\ v_{R1} \end{bmatrix} + B_0\lambda_2^n\begin{bmatrix} v_{I2} \\ v_{R2} \end{bmatrix}, \quad (8)$$

where A_0 and B_0 are complex constants determined by boundary conditions. The end boundary conditions with reflection coefficient α give

$$\frac{R_n e^{jk(x-x_n+\omega t)}}{I_n e^{-jk(x-x_n-\omega t)}} = \frac{A_0{\lambda_1}^{n-1}v_{R1}e^{jkL_{end}} + B_0{\lambda_1}^{n-1}v_{R2}e^{jkL_{end}}}{A_0{\lambda_1}^{n-1}v_{I1}e^{-jkL_{end}} + B_0{\lambda_1}^{n-1}v_{I2}e^{-jkL_{end}}} = \alpha. \quad (9)$$

Similarly, the initial condition gives

$$\begin{aligned} p_0 &= I_0 e^{-jk(x+d)} + R_0 e^{jk(x+d)}|_{x=-L_{start}} \\ &= (A_0{\lambda_1}^{-1}v_{I1} + B_0{\lambda_2}^{-1}v_{I2})e^{-jk(d-L_{start})} + (A_0{\lambda_1}^{-1}v_{R1} + B_0{\lambda_2}^{-1}v_{R2})e^{jk(d-L_{start})}. \end{aligned} \quad (10)$$

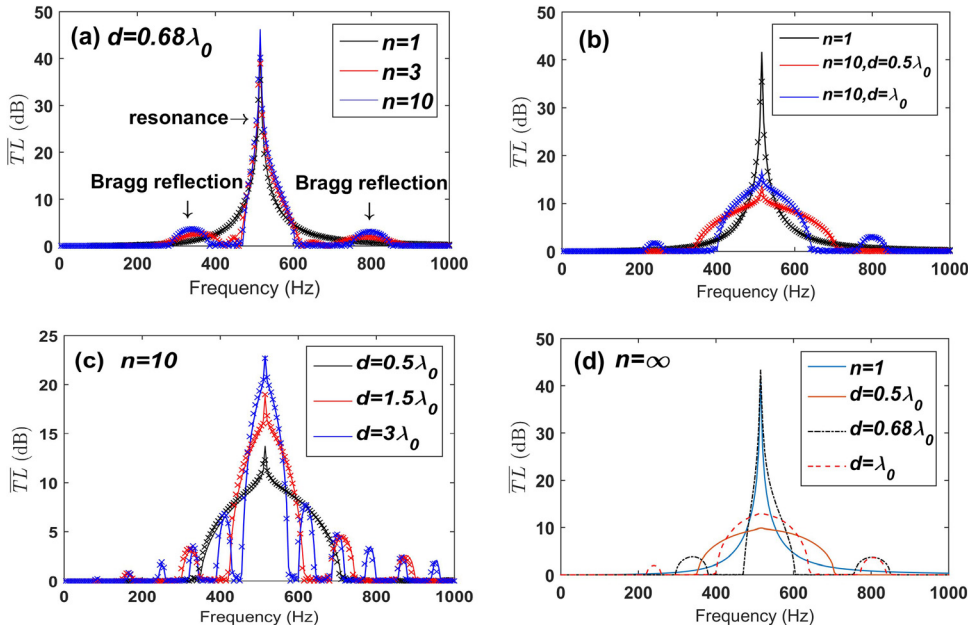

Fig. 2. (Color online) The average transmission loss $\overline{TL}$ of the duct resonator system with different numbers of resonators $(n+1)$ or periodic distances (d). Lines represent theoretical results and dotted crosses represent FEM simulations.

Thus the average transmission loss can be expressed as

$$\overline{TL} = \frac{20}{n+1}\log_{10}\left|\frac{I_0}{I_{n+1}}\right| = \frac{20}{n+1}\log_{10}\left|\frac{A_0\lambda_1{}^{-1}v_{I1} + B_0\lambda_2{}^{-1}v_{I2}}{A_0\lambda_1{}^{n-1}v_{I1} + B_0\lambda_2{}^{n-1}v_{I2}}\right|. \tag{11}$$

When the duct ends with an anechoic termination, the reflection α equals zero, and λ_1 describes positive-direction propagation, it means that $|\lambda_1| < 1$, $|\lambda_2| > 1$. $B_0 = 0$ is required in this situation. The average transmission loss of a duct with an anechoic termination loaded with infinity resonators can be expressed as $\overline{TL} = -20\log_{10}|\lambda_1|$.

3.2 Helmholtz resonators' sound power storage capacity

The transmission loss index is only used to evaluate acoustic transmission performance. A parameter based on the transmission loss index is first proposed here to investigate HRs' energy storage capacity. According to the definition of the transmission loss,[3]

Table 1. $\overline{TL}$ area and W_{total} of a periodic ducted HR system with different numbers of HR.

	$d = 0.5\lambda$				$d = \lambda$			
	Theory		FEM		Theory		FEM	
Resonator number	$\overline{TL}$ area ($\times 10^3$)	W_{total} ($\times 10^{-4}$)	$\overline{TL}$ area ($\times 10^3$)	W_{total} ($\times 10^{-4}$)	$\overline{TL}$ area ($\times 10^3$)	W_{total} ($\times 10^{-4}$)	$\overline{TL}$ area ($\times 10^3$)	W_{total} ($\times 10^{-4}$)
1	2.6766	2.4333	2.7532	2.5108	2.6766	2.4333	2.7532	2.5108
2	2.6562	2.5203	2.7378	2.5097	2.6654	2.5055	2.7445	2.5078
3	2.6422	2.5198	2.7272	2.5041	2.6596	2.4889	2.7396	2.5041
4	2.6337	2.5	2.7205	2.4987	2.6576	2.4745	2.7347	2.4958
5	2.6288	2.4845	2.7161	2.4954	2.6576	2.4743	2.7361	2.5022
6	2.6263	2.4742	2.7133	2.5002	2.6575	2.4695	2.7353	2.5001
7	2.6254	2.4678	2.7117	2.4932	2.6569	2.4652	2.7373	2.5256
8	2.6253	2.4362	2.71	2.4812	2.6565	2.4618	2.7378	2.5385
9	2.6252	2.4602	2.711	2.4798	2.6565	2.4617	2.7351	2.4995
10	2.6249	2.4567	2.7092	2.4631	2.6565	2.4618	2.7329	2.4887
12	2.6237	2.4496	2.7086	2.4569	2.6563	2.4592	2.7249	2.4754
16	2.6222	2.4406	2.7086	2.4569	2.6563	2.4595	2.7376	2.5002
24	2.6211	2.4313	2.703	2.4471	2.656	2.4564	2.7315	2.4841
32	2.6209	2.4272	2.7043	2.4521	2.6555	2.4552	2.7424	2.5012
48	2.6198	2.4237	2.7042	2.4536	2.6555	2.457	2.7469	2.5056
64	2.6201	2.4195	2.7077	2.4468	2.6554	2.4571	2.7536	2.5263

Table 2. $\overline{TL}$ area and W_{total} of ten HR duct resonators with different periodic distances.

	Periodic d	0.5λ	λ	1.5λ	2λ	2.5λ	3λ	3.5λ
FEM	$\overline{TL}$ area ($\times 10^3$)	2.7092	2.7329	2.7364	2.747	2.7389	2.754	2.752
	W_{total} ($\times 10^{-4}$)	2.4631	2.4887	2.503	2.5123	2.4986	2.5206	2.5065
Theory	$\overline{TL}$ area ($\times 10^3$)	2.6249	2.6565	2.6672	2.6729	2.6767	2.6795	2.6807
	W_{total} ($\times 10^{-4}$)	2.4567	2.4618	2.4695	2.4853	2.5069	2.5098	2.5104

$$TL = Lw_i - Lw_t = 10\lg(w_i/w_t), \tag{12}$$

where $w_i = S_i|p_i|^2/\rho c$ and $w_t = S_t|p_t|^2/\rho c$ are the incident sound power and transmission sound power, respectively. Since HRs are reactive silencers without energy consumption, their energy storage capacity in a frequency domain is expressed as

$$W_{total} = \int (w_i - w_t) = \int (w_i - w_i/10^{TL/10}) = \sum_{1}^{fr} (w_i - w_i/10^{TL_{fr}/10}). \tag{13}$$

When the dimensions of a duct resonator system and the incident sound power are determined, HRs' energy storage capacity remains unchanged. The periodic distance only affects stopbands' position, bandwidth, and amplitude; however, it has no effect on HRs' energy storage capacity. Owing to multiple relationships between the integration of the $\overline{TL}$ curve or W_{total} in a frequency domain, the integration of $\overline{TL}$ curves can be used to evaluate HRs' energy storage capacity and noise control optimization design.

4. Results and discussion

A duct resonator system with the geometries $S_d = 36$ cm^2, $l_n = 2.5$ cm, $S_n = 4\pi$ cm^2, and $V = 101.25\pi$ cm^3 was used in this study. The three-dimensional finite method was used to validate theoretical prediction. An oscillating sound pressure at a magnitude of $P_0 = 1$ was applied at the beginning of the duct. An anechoic termination was set at the end to avoid reflected waves.

Figure 2(a) shows $\omega_0 \neq \omega_m$ cases ($n = 1, 3, 10$) with two types of stopband separately. The $\overline{TL}$ of two different special cases ($\omega_0 = \omega_1 = \pi d$ and $\omega_0 = \omega_m = 2\pi d$) was compared with a single-branch HR in Fig. 2(b), in which the stopband near the resonance frequency is a combination of Bragg reflection and resonance effect. The relationship between integer number m and periodic distance d in special cases is given as $d = m\lambda_0/2$. Figure 2(c) shows that the width of the stopband becomes narrower as $\sqrt{1/m}$ with increasing m in special cases ($d = 0.5\lambda_0, 1.5\lambda_0, 3\lambda_0$). Thus, for the sake of having a broader stopband at resonance frequency, $d = \lambda_0/2 (m = 1)$ is often chosen as periodic distance. Figure 2(d) verifies $\overline{TL} = -20\log_{10}|\lambda_1|$ in cases of infinite resonators, and also compares three different cases ($d = 0.5\lambda_0, 0.68\lambda_0, \lambda_0$) with a single-branch HR. The theoretical $\overline{TL}$ of different cases shown in Fig. 2 are compared with the numerical simulation using three-dimensional finite element methods (FEMs) (dotted crosses). The predicted result fits well with the FEM results. In addition, the results illustrate that the broader the noise attenuation band, the lower the peak attenuation amplitude.

Based on the conservation of energy, the total energy W_{total} of all $\overline{TL}$ curves (summation of the power spectral of $\overline{TL}$) from 0 to 1000 Hz are almost the same, as is the area covered by $\overline{TL}$ curves. Tables 1 and 2 show different cases with different periodic distances and numbers of resonators by both theoretical prediction and simulation. The maximum relative error of $\overline{TL}$ area and W_{total} between theoretical analysis

Table 3. Relative error between the minimum value and maximum value.

	Theory		FEM	
	Min	Max	Min	Max
Case	48 HRs, 0.5λ	10 HRs, 3.5λ	24 HRs, 0.5λ	10 HRs, 3λ
$\overline{TL}$ area ($\times 10^3$)	T1 = 2.6198	T2 = 2.6907	T3 = 2.703	T4 = 2.754
Case	64 HRs, 0.5λ	2 HRs, 0.5λ	64 HRs, 0.5λ	8 HRs, λ
W_{total} ($\times 10^{-4}$)	T5 = 2.4195	T6 = 2.5203	T7 = 2.4468	T8 = 2.5385
Relative error (%)	T1/ T2: 2.6%; T3/ T4: 1.9%; T1/ T4: 4.9%; T5/ T6: 4%; T7/ T8: 3.6%; T5/T8: 4.7%			

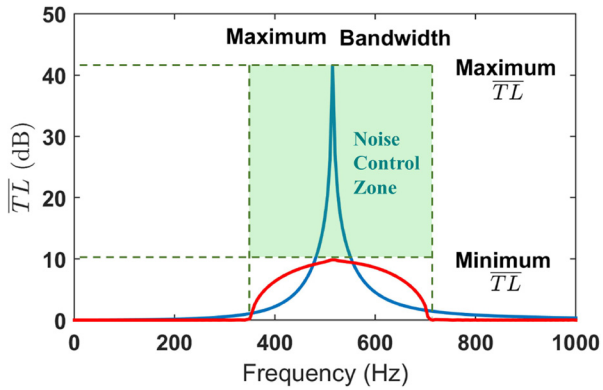

Fig. 3. (Color online) Noise control zone for ducted HRs.

and FEM are 3.6% (case: 64 HRs with distance λ) and 3.1% (case: single HR), respectively.

The relative errors between the minimum value and the maximum value are exhibited in Table 3. These three tables indicate that for the same system, no matter how many HRs are used or what the periodic distance is, the $\overline{TL}$ area and W_{total} are always the same. This means that HR's noise attenuation capacity remains the same for the same geometries of duct and resonator.

There is no trick to noise control. The broader the noise attenuation band, the lower the peak attenuation amplitude. Although different $\overline{TL}$ curves with different bandwidths and peak amplitudes could be obtained with different periodic distances, $\overline{TL}$ area and W_{total} are always the same and $\overline{TL}$ curves always fall into the boundaries of a noise control zone. The noise control zone as shown in Fig. 3 is first proposed for noise control optimization design. It provides a clear indication of the limitation of noise control. No matter what optimizing distance[8–10] is adopted in noise control, the values of the attenuation bandwidth and peak amplitude must be within the proposed noise control zone. The noise control zone can be used to analyze the feasibility of desired broad attenuation bandwidth and peak amplitude in noise control optimization. Figure 3 shows the noise control zone for periodic ducted HRs, which is bounded by the highest $\overline{TL}$ amplitude for a single resonator, and has the largest frequency bandwidth with lowest $\overline{TL}$ amplitude for $d = \lambda_0/2$.

5. Conclusion

This paper presents a theoretical study of the dispersion characteristics of sound wave propagation in a periodic ducted HR system. The predicted result fits well with the FEM results. This study indicates that for the same system, no matter how many HRs are connected or what the periodic distance is, the $\overline{TL}$ area and W_{total} are always the same. In other words, changing the resonator number or the value of the periodic distance has no effect on the HR's noise attenuation capacity. The broader the noise attenuation band the lower the peak attenuation amplitude. A noise control zone compromising the attenuation bandwidth or peak amplitude is first proposed to illustrate the limitation of noise control for a ducted HR system and can be used to analyze the feasibility of desired broad attenuation bandwidth and peak amplitude in noise control optimization. $\overline{TL}$ curves always fall into the boundaries of the noise control zone as long as the geometries of the duct resonator are the same. Optimal transmission loss can be obtained by taking full advantage of periodicity and noise control zone in the design, achieving the required noise attenuation band and peak attenuation amplitude.

Acknowledgments

The work described in this paper was fully supported by a grant from the Research Grants Council of the Hong Kong Special Administrative Region, China (Project No. PolyU 152116/14E).

References and links

[1]J. W. S. Rayleigh, *The Theory of Sound*, 2nd ed. (Dover, New York, 1945), Vol. II.
[2]U. Ingard, "On the theory and design of acoustic resonators," J. Acoust. Soc. Am. **25**, 1037–1061 (1953).
[3]M. L. Munjal, *Acoustics of Ducts and Mufflers* (Wiley, New York, 1987).
[4]P. K. Tang and W. A. Sirignano, "Theory of a generalized Helmholtz resonator," J. Sound Vib. **26**(2), 247–262 (1973).

[5]A. Selamet and N. S. Dickey, "Theoretical, computational, and experimental investigation of Helmholtz resonators with fixed volume: Lumped versus distributed analysis," J. Sound Vib. **187**(2), 358–367 (1995).
[6]X. Wang and C. M. Mak, "Wave propagation in a duct with a periodic Helmholtz resonators array," J. Acoust. Soc. Am. **131**(2), 1172–1182 (2012).
[7]R. A. Prydz, L. S. Wirt, and H. L. Kuntz, "Transmission loss of a multilayer panel with internal tuned Helmholtz resonators," J. Acoust. Soc. Am. **87**, 1597–1602 (1990).
[8]A. Trochidis, "Sound transmission in a duct with an array of lined resonators," J. Vib. Acoust. **113**, 245–249 (1991).
[9]S. H. Seo and Y. H. Kim, "Silencer design by using array resonators for low-frequency band nose reduction," J. Acoust. Soc. Am. **118**(4), 2332–2338 (2005).
[10]O. Richoux, B. Lombard, and J.-F. Mercier, "Generation of acoustic solitary waves in a lattice of Helmholtz resonators," J. Wave Motion. **56**, 85–99 (2015).
[11]N. Sugimoto and T. Horioka, "Dispersion characteristics of sound waves in a tunnel with an array of Helmholtz resonators," J. Acoust. Soc. Am. **97**(3), 1446–1459 (1995).
[12]X. Wang and C. M. Mak, "Acoustic performance of a duct loaded with identical resonators," J. Acoust. Soc. Am. **131**(4), EL316–EL322 (2012).
[13]C. E. Bradley, "Time harmonic acoustic Bloch wave propagation in periodic waveguides. Part I. Theory," J. Acoust. Soc. Am. **96**, 1844–1953 (1994).